



Dual electrocatalysis enables enantioselective hydrocyanation of conjugated alkenes

Lu Song¹, Niankai Fu¹, Brian G. Ernst¹, Wai Hang Lee¹, Michael O. Frederick², Robert A. DiStasio Jr.¹ and Song Lin¹

Chiral nitriles and their derivatives are prevalent in pharmaceuticals and bioactive compounds. Enantioselective alkene hydrocyanation represents a convenient and efficient approach for synthesizing these molecules. However, a generally applicable method featuring a broad substrate scope and high functional group tolerance remains elusive. Here, we address this long-standing synthetic problem using dual electrocatalysis. Using this strategy, we leverage electrochemistry to seamlessly combine two canonical radical reactions—cobalt-mediated hydrogen-atom transfer and copper-promoted radical cyanation—to accomplish highly enantioselective hydrocyanation without the need for stoichiometric oxidants. We also harness electrochemistry's unique feature of precise potential control to optimize the chemoselectivity of challenging substrates. Computational analysis uncovers the origin of enantio-induction, for which the chiral catalyst imparts a combination of attractive and repulsive non-covalent interactions to direct the enantio-determining C-CN bond formation. This work demonstrates the power of electrochemistry in accessing new chemical space and providing solutions to pertinent challenges in synthetic chemistry.

Alkene hydrocyanation, in which H and CN groups are added across a C=C π -bond, is a highly useful transformation^{1–4}, as it provides versatile nitriles that are key intermediates in the synthesis of polymers, agrochemicals, cosmetics and pharmaceuticals (Fig. 1a)⁵. This reaction is used in the industrial production of adiponitrile on a million-tonne annual scale⁶ and has been explored by scientists at DuPont in the synthesis of naproxen, a top-selling anti-inflammatory medicine^{7–9}. The development of a general catalytic alkene hydrocyanation method with broad substrate scope, precise chemoselectivity and high stereochemical control would have a substantial impact on synthetic organic chemistry across both academia and industry. Despite extensive studies on the enantioselective hydrocyanation of polar π -bonds (for example, C=O and C=N)¹⁰, analogous methods for the hydrocyanation of alkenes remain underdeveloped¹¹. Following early examples of highly enantioselective hydrocyanation of 2-methoxy-6-vinylnaphthalene by RajanBabu et al. in the context of naproxen synthesis^{7–9}, seminal contributions have been made using transition metal catalysis (for example, Ni catalysis; Fig. 1b)^{12–17}. To date, however, a general catalytic approach that meets the criteria of both broad reaction scope and high enantioselectivity remains elusive. In particular, internal alkenes, which would lead to a substantially wider range of useful products, have proven to be challenging substrates.

Recently, we have established electrocatalysis^{18–21} as a broadly applicable strategy for the difunctionalization of alkenes²². This approach merges the electrochemical generation of radical intermediates with catalyst-controlled radical addition to the alkene. Specifically, we devised anodically coupled electrolysis—a process that combines two anodic events to form two distinct radical intermediates—for the synthesis of a diverse suite of vicinally heterodifunctionalized structures^{23,24}. Further applying electrocatalysis to the hydrofunctionalization of alkenes, such as hydrocyanation, would substantially expand the scope of electro-synthesis. Such transformations would enable direct access to a

specific monofunctionalized product in one step from the alkene precursor, and are therefore complementary to difunctionalization reactions in the context of target-oriented synthesis. Achieving this reaction enantioselectively would further increase its synthetic value and grant access to valuable chiral targets for applications in organic synthesis and medicinal chemistry. Early studies in electro-organic synthesis demonstrated the feasibility of electrochemical hydrofunctionalization of alkenes. However, known examples are primarily limited to intramolecular cyclizations²⁵ or reactions using activated alkenes (for example, Michael acceptors)²⁶ with limited examples of intermolecular hydrofunctionalization of unactivated alkenes²⁷. In addition, no enantioselective variants are currently available. In general, electrosynthetic methods that enable asymmetric alkene functionalization remain elusive^{28–30}. Against this backdrop, we describe an electrochemical approach for the enantioselective hydrocyanation of conjugated alkenes powered by a Co/Cu dual electrocatalytic process.

Results and discussion

Reaction design. Achieving the desired hydrocyanation using our electrocatalytic strategy would require the parallel generation of two open-shell species that serve as H[•] and CN[•] equivalents. Towards this goal, we envisioned combining two metal-mediated elementary radical reactions in an anodically coupled electrocatalytic system (Fig. 2a). In the proposed catalytic cycle, [Co^{III}]-H (formally), generated from a Co^{III} precursor and a hydrosilane^{31–35}, reacts with an alkene substrate via hydrogen-atom transfer (HAT) to produce carbon-centred radical **I**^{36–38}. This intermediate then enters the cyanation cycle and undergoes single-electron oxidative addition to [Cu^I]-CN to form species **II**, a formally Cu^{III} intermediate. Subsequent reductive elimination completes the hydrocyanation reaction^{39–41}.

This reaction design has garnered inspiration from two key discoveries in the area of metal-mediated radical chemistry. For one,

¹Department of Chemistry and Chemical Biology, Cornell University, Ithaca, NY, USA. ²Small Molecule Design and Development, Eli Lilly and Company, Indianapolis, IN, USA. ✉e-mail: distasio@cornell.edu; songlin@cornell.edu

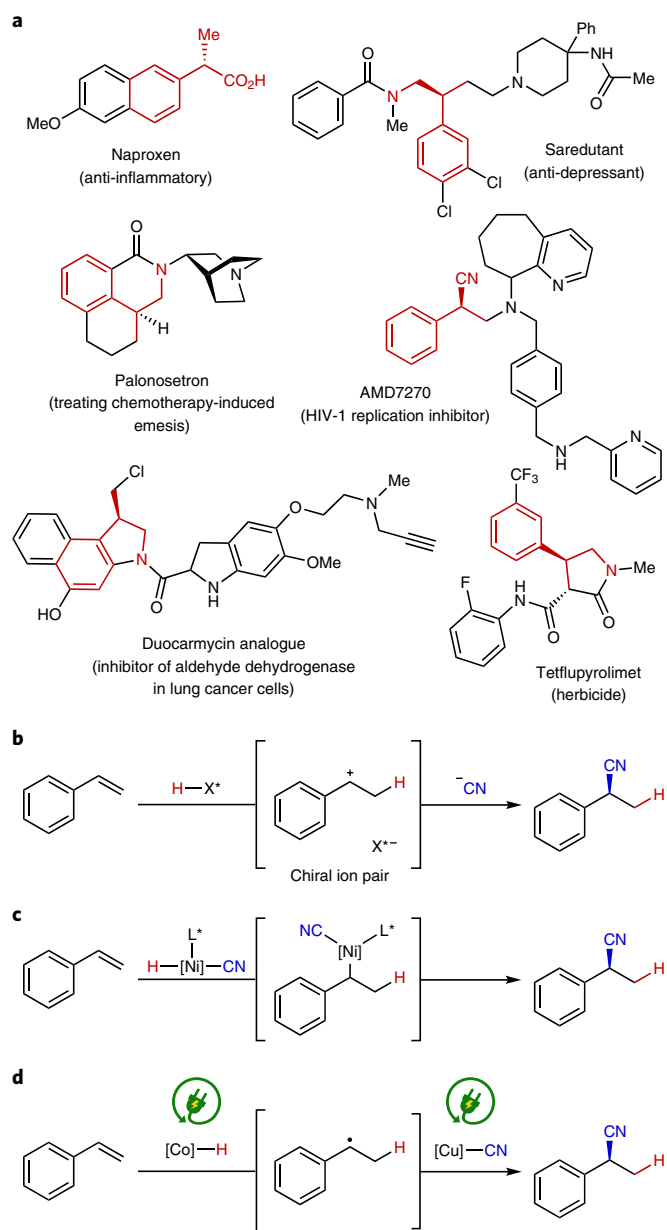


Fig. 1 | Enantioselective hydrocyanation: synthetic significance and proposed strategy. **a**, Arylpropionitriles and derivatives in pharmaceuticals and agrochemicals. **b–d**, Strategies for enantioselective hydrocyanation of alkenes. A challenge for the carbocation pathway (**b**) is that enantio-induction with benzyl cations is difficult. There are no precedents, despite extensive use of this strategy in C=X (X = O, N) hydrocyanation¹⁰. Challenges for the Ni hydride pathway (**c**) are the limited scope and the fact that the reaction yield and selectivity are highly dependent on the structure and electronic properties of the alkene. There are precedents to this pathway^{7–9,12–15}. Features of the electrochemical radical pathway (**d**) in this work are its broad scope, high enantioselectivity, high functional group tolerance, electrochemical control of chemoselectivity and mechanistic information. Asterisks in **b–d** denote chiral groups or ligands.

metal hydride hydrogen-atom transfer (MHAT) has recently been established as a versatile approach for the hydrofunctionalization of alkenes³¹. Directly related to this work, Carreira reported a racemic version of Co-catalysed alkene hydrocyanation using TsCN as the CN source³. Recently, Shenvi showed for the first time that

HAT-initiated alkene functionalization could intercept a second organometallic cycle in the context of Co/Ni-catalysed hydroarylation⁴². Nevertheless, there have been very few applications of MHAT to asymmetric catalysis⁴³, and no study has been performed to date in the context of MHAT-mediated electrocatalysis. Secondly, our mechanistic design was also inspired by recent advances in enantioselective Cu-catalysed radical cyanation. For example, Liu reported a series of elegant methods for the enantioselective cyanofunctionalization of styrenes promoted by chemical oxidants⁴⁰. Harnessing this reactivity, we have recently established the viability of Cu-mediated asymmetric electrocatalysis in the context of cyanophosphinoylation of alkenes by replacing chemical oxidants⁴⁴ with an anode⁴⁵. However, the scope of this cyanophosphinoylation reaction was limited to terminal styrenes. More importantly, Cu catalysis alone is not amenable to the development of a highly enantioselective hydrocyanation reaction, which is a synthetically more valuable transformation. In this work, we investigate a dual catalytic strategy that harnesses the synergistic combination of Co HAT and Cu cyanation, thereby providing a unique solution to this synthetic challenge.

The desired hydrocyanation reaction is an overall oxidative transformation, which requires the turnover of both catalysts via a pair of single-electron oxidation events to return the resultant Co^{II} and Cu^I species back to their reactive Co^{III} and Cu^{II} oxidation states (Fig. 2a). The key to successfully achieving this reaction therefore relies on the identification of oxidative conditions that seamlessly accommodate both the Co HAT and Cu cyanation cycles. We note that the attributes of electrochemistry render it uniquely capable of facilitating the merger of these two catalytic processes into a broadly useful hydrocyanation protocol. On one hand, Co-catalysed hydrofunctionalization can encounter chemoselectivity issues with styrene-type substrates (vide infra), particularly in the presence of an oxidant; this is likely due to the formation of a benzylic radical that is susceptible to over-oxidation to a benzyl cation⁴⁶. On the other hand, Cu-catalysed cyanation requires a potent chemical oxidant^{39,40}, which can also limit the reaction scope to substrates lacking oxidatively labile functional groups. By contrast, electrochemical strategies allow one to dial in a minimally sufficient potential, thereby circumventing the need for stoichiometric oxidants and addressing the incompatibility issues potentially associated with our Co/Cu dual catalytic process.

Reaction discovery and development. We set out to evaluate various combinations of Co and Cu catalysts. The electrochemical properties of many Co complexes have been well documented⁴⁷. However, the electrochemical compatibility and behaviour of Cu complexes with common chiral ligands are largely unknown. In addition, Cu ions are highly susceptible to electroplating on the cathode (complete reduction of Cu(OTf)₂ observed at approximately –0.5 V versus ferrocenium/ferrocene, Fc^{+/0}, in dimethylformamide (DMF); see Supplementary Fig. 8). In an undivided electrochemical cell (for example, a standard laboratory flask), an ideal vessel for preparative-scale electrochemical reactions, Cu complexes could be readily reduced at the cathode and lose catalytic activity⁴⁸. Through systematic optimization, we found that Co(salen) complex **3** (0.5 mol%) and Cu(OTf)₂ (5 mol%) together with bisoxazoline (BOX)-type ligands (**5–7**; 10 mol%) in the presence of PhSiH₃ and trimethylsilyl cyanide (TMSCN) promoted the conversion of 4-*tert*-butylstyrene (**1**) to the desired product (**2**) in good yield and moderate enantioselectivity (50–72% e.e.; Fig. 2b). Cyclic voltammetry studies revealed that both the BOX ligand and CN[–] are important in keeping the Cu catalyst in solution presumably through the formation of [Cu(BOX)(CN)_{*n*}]-type complexes, avoiding detrimental cathodic deposition during electrolysis (see Supplementary Fig. 9). In addition, the combination

of Pt as the cathode and HOAc as the terminal oxidant is important to ensure facile proton reduction at a relatively low overpotential, which outcompetes the undesired Cu reduction.

To further optimize enantioselectivity, we surveyed a catalogue of chiral bidentate *N,N*- and *P,P*-ligands, including several that are known to be excellent Cu ligands for enantioselective Lewis acid⁴⁹ or radical catalysis^{39,40,50,51}. However, the optimal e.e. could not be improved above 72% (ligand 7). During our reaction optimization, we discovered that serine-derived bisoxazolines (sBOXs; for example, 4) are excellent ligands in the desired hydrocyanation reaction. These ligands are readily prepared from serine⁵², and were recently shown by us to be effective ligands in the cyanophosphinoylation reaction as well⁴⁵. As shown in Fig. 2b, the use of ligand 4 drastically improved the reaction enantioselectivity to 91% e.e. and also increased the yield to 79%. Using computational methods, we show that such high reaction enantioselectivity arises from a complex interplay between attractive and repulsive non-covalent interactions due to the second-sphere ester groups in these sBOX ligands (vide infra).

A number of control experiments serve to highlight the importance of each component of our reaction system. For example, using MeCN instead of DMF as the solvent, LiClO₄ instead of tetrabutylammonium tetrafluoroborate (TBABF₄) as the electrolyte or EtOH instead of HOAc as the proton source led to decreased product yield (Fig. 2b). Notably, the product was also formed in substantially lower e.e. in the presence of LiClO₄. Previous work showed that the identity of the electrolyte can substantially affect the polarity of the electrical double layer (EDL)⁵³. As such, we hypothesize that TBABF₄ creates a much less polar EDL on the anode than LiClO₄, which is responsible for the improved enantioselectivity. When Co loading was increased from 0.5 to 2 mol%, the yield of 2 was dramatically decreased and a large amount of hydrogenated side product was observed³⁸. This result highlights the importance of balancing the rates of the HAT and cyanation events to ensure optimal product selectivity. Finally, the reaction requires both Cu and Co to operate, as excluding either catalyst led to minimal conversion to the hydrocyanation product.

Reaction scope and application. In addition to representing a conceptual advance, our electrochemical hydrocyanation is also synthetically valuable and provides a complementary route to existing methods for the synthesis of chiral nitriles. Under optimal conditions, a variety of vinylarenes underwent hydrocyanation to furnish desired arylpropionitriles with excellent enantioselectivity (Table 1). The efficiency of the transformation was found to be relatively independent of the electronic properties of the aryl substituents. Importantly, the very mild reaction conditions imparted by the combination of electrochemistry and a radical mechanism made accessible a broad scope of enantio-enriched nitriles with a diverse range of functional groups. In particular, functionalities that are susceptible to oxidative degradation under chemical conditions, such as electron-rich arenes (for example, 8, 15, 20), sulfides (11) and aldehydes (13), can be readily engaged in the hydrocyanation. Furthermore, groups including benzyl chlorides (12), aryl halides (9, 25) and aryl boronates (17), which might induce catalyst promiscuity under Ni-promoted conditions, were well tolerated in our reaction. Alkenes with various heterocycles (20–23, 25) also proved excellent substrates. The scalability of the reaction was demonstrated in the synthesis of products 2 and 15 on 2–5 mmol scales (a 10–25 times scale-up), which were isolated in comparable but marginally decreased yield and e.e. We attribute the reduction in yield and e.e. to inefficient mass and heat transport due to the heterogeneous nature of electrode reactions, which may be addressed via reactor engineering.

Our reaction is also applicable to internal alkenylarenes (Table 1), which are typically challenging substrates in previously

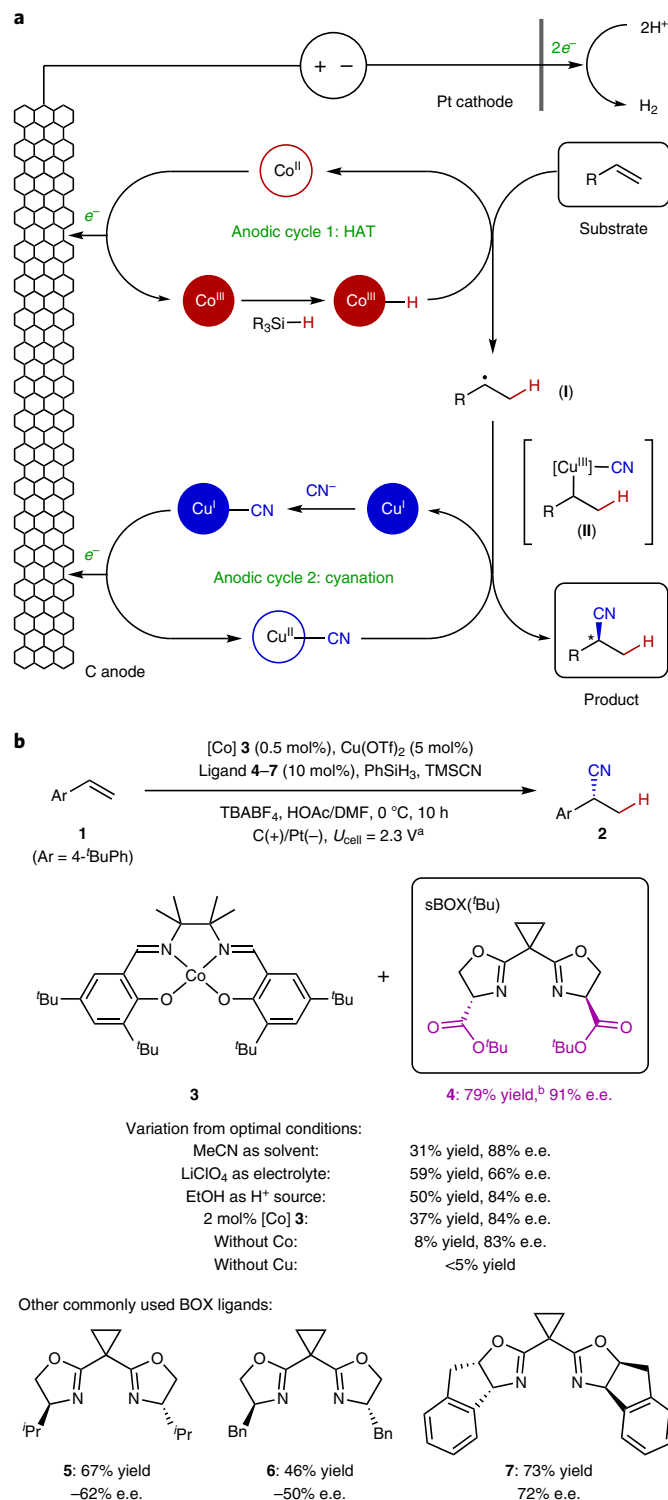
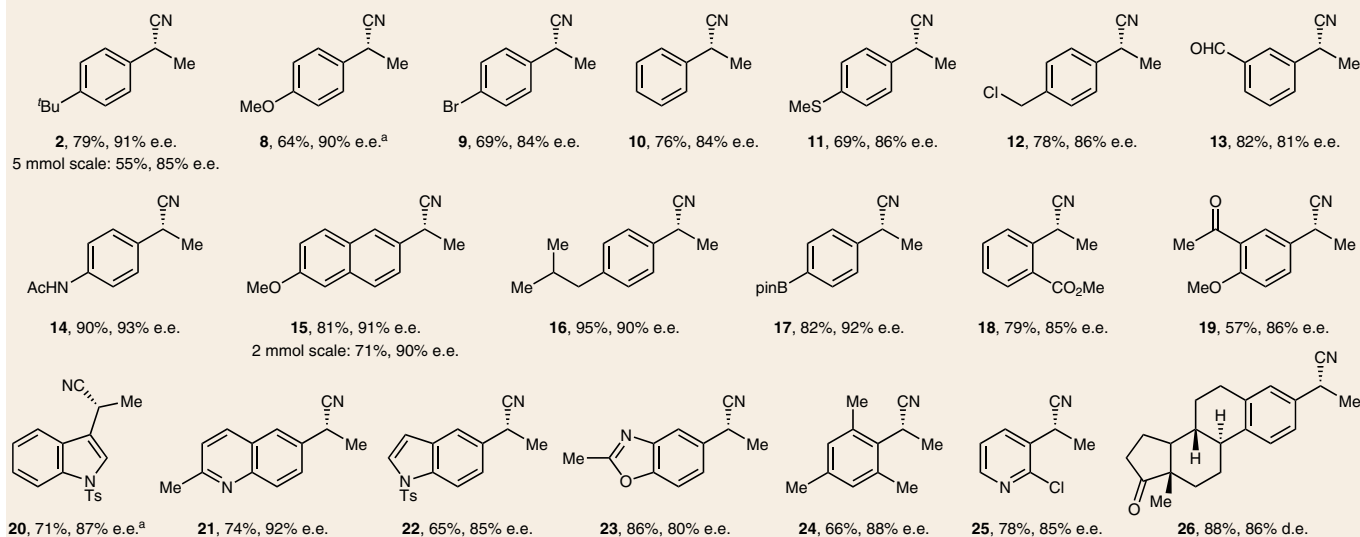


Fig. 2 | Reaction design, discovery and optimization. **a**, Anodically coupled dual electrocatalysis provides an effective strategy to couple two distinct radical catalytic cycles for alkene hydrocyanation. **b**, Optimization of the reaction conditions and control experiments. Yields were determined by ¹H NMR. ^aU_{cell}, cell voltage applied between the cathode and anode; U_{cell} = 2.3 V corresponds to -0.24 V versus Fc^{+/0} anodic potential (E_{anode}) and gives -2 mA initial current. ^bIsolated yield. e.e., enantiomeric excess.

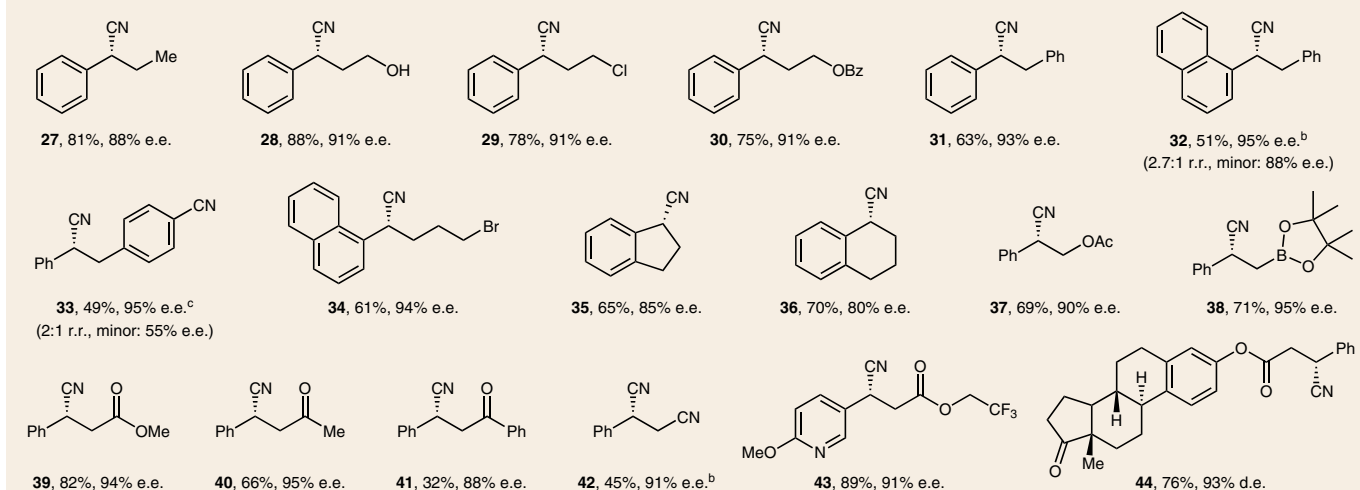
reported enantioselective hydrocyanation reactions due to their low reactivity¹³. Our protocol shows very broad substrate generality, furnishing products with a variety of synthetically useful

Table 1 | Reaction scope

Terminal alkenes:

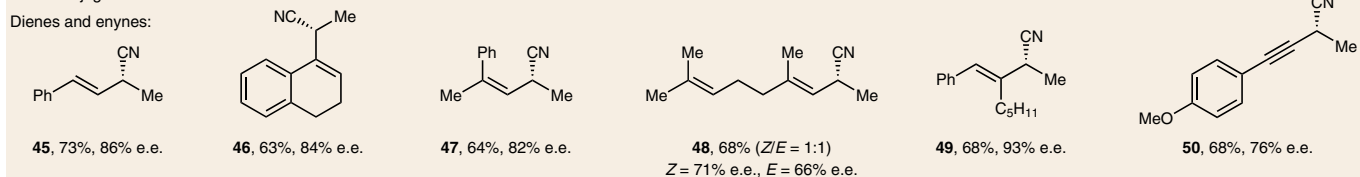


Internal alkenes:

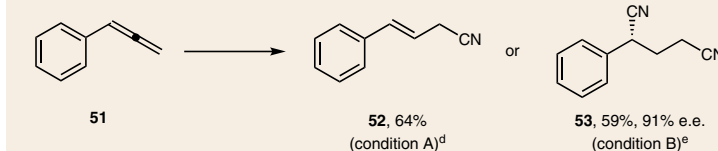


Other conjugated alkenes:

Dienes and enynes:



Allene:



Radical probe:



Conditions: alkene (0.2 mmol, 1 equiv.), PhSiH₃ (1.1 equiv.), TMSCN (2.0 equiv.), Co **3** (0.5 mol%), Cu(OTf)₂ (5 mol%), ligand **4** (10 mol%), TBABF₄ (2.0 equiv.), HOAc (5.0 equiv.), DMF (4.0 ml), C anode, Pt cathode, undivided cell, 0 °C and *U*_{cell} = 2.3 V. Isolated yields are reported, unless otherwise noted. ^aOptimal yield obtained at *U*_{cell} = 1.8 V (see Fig. 4a and corresponding discussion). ^bWith 1 mol% Co **3**. ^cWith 2 mol% Co **3**. ^dCondition A: with 1.5 equiv. TMSCN, 1.1 equiv. PhSiH₃; yield determined by ¹H NMR. ^eCondition B: with 4.0 equiv. TMSCN, 2.2 equiv. PhSiH₃. r.r., regiomer ratio; d.e., diastereomeric excess.

functional handles (**28**, **29**, **34**, **38**) and N-heterocyclic motifs (**43**). Since the stereochemistry of the starting alkene does not affect the yield or enantioselectivity, a mixture of *E* and *Z* isomers

can be used directly in this reaction. Both electron-rich (**37**) and electron-deficient (**39–44**) alkenes proved suitable substrates. In particular, hydrocyanation was achieved for cinnamoyl-type

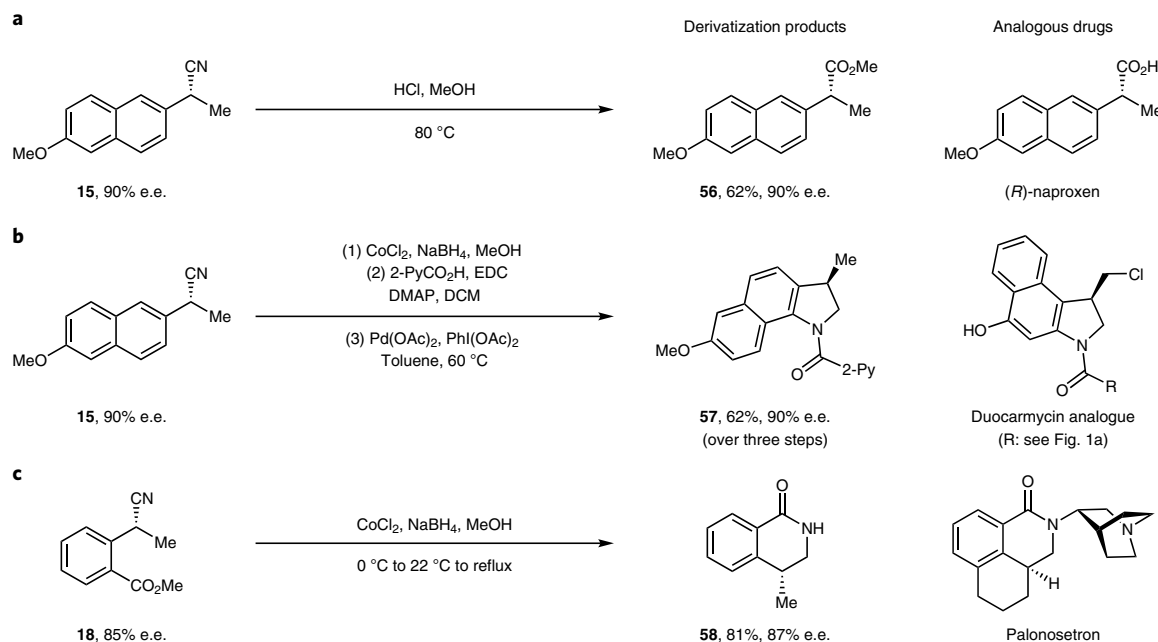


Fig. 3 | Product derivatization. **a**, Product **15** is transformed to naproxen methyl ester **56** (analogue of naproxen) via methanolysis. **b**, Product **15** is transformed to benzoin derivative **57** (analogue of duocarmycin) via reduction followed by C–H amination. **c**, Product **18** is transformed to dihydroisoquinolone **58** (analogue of palonosetron) via reduction and subsequent amide formation. Detailed experimental procedures can be found in Section 6 of the Supplementary Information. DMAP, 4-(dimethylamino)pyridine; EDC, 1-(3-dimethylaminopropyl)-3-ethylcarbodiimide hydrochloride; DCM, dichloromethane.

structures including esters (**39**, **43**, **44**), ketones (**40**, **41**) and nitriles (**42**). These results demonstrate that our reaction can serve as a more general alternative to the enantioselective Michael addition en route to similar products. Considering that numerous bioactive natural products and their synthetic precursors contain cinnamoyl side chains (for example, taxol, phyllanthocin), our method provides a convenient means to derivatize these compounds for medicinal chemistry studies.

We further extended the scope of our reaction to other types of unsaturated substrates (Table 1). For example, dienes were converted to mono-hydrocyanated products in high efficiency and enantioselectivity. In the case of linear dienes (**45**–**49**), the reaction selectively functionalizes the terminal C=C π -bond. Structurally analogous enynes also reacted chemoselectively in good e.e. (**50**). Interestingly, in these transformations, enantioselective Cu-mediated C–CN bond formation is achieved via an allyl or propargyl radical species⁵⁴. Finally, we expanded the reaction scope to allenes. The hydrocyanation of phenylallene (**51**) yielded cinnamyl cyanide (**52**) as the predominant product. Based on density functional theory (DFT) calculations, we believe that this product arose from regioselective HAT at the central allene carbon to form an allyl radical (24.3 kcal mol⁻¹ more stable than the corresponding vinyl radical; see Supplementary Fig. 13) followed by Cu-promoted regioselective cyanation at the primary carbon to maintain the conjugated styrene motif (4.1 kcal mol⁻¹ lower barrier than cyanation at the benzylic carbon; see Supplementary Fig. 13). This selectivity allowed us to achieve double hydrocyanation through the use of an excess of reagents to generate 1,3-dinitrile **53** with high enantioselectivity. A radical rearrangement experiment provided key support for the intermediacy of the organic radical species. Exposure of cyclopropane-derived alkene **54** to the reaction conditions led to the expected ring opening, furnishing alkene-containing nitrile **55** in high yield and enantioselectivity.

Alkyl nitriles are highly versatile synthetic intermediates that can be readily transformed to a variety of useful functional groups, such as aldehydes, alcohols, carboxylic acids, esters, amines and heterocycles. Here we showcase the synthetic value of our reaction products through three examples (Fig. 3). Product **15** was readily converted to either naproxen methyl ester **56** via methanolysis or to benzoin derivative **57** via reduction followed by Pd-catalysed C–H amination⁵⁵. Both derivatizations occurred with complete retention of stereochemistry. Nitrile **18** was subjected to reduction and subsequent cyclization to yield dihydroisoquinolone **58**. These products bear structural resemblance to high-value drug molecules, again highlighting the significance of the enantioselective hydrocyanation reaction.

Electrochemical control of reaction chemoselectivity. A key advantage of electrochemistry is the ability to achieve external control over the electrode potential input. This feature allowed us to regulate the hydrocyanation chemoselectivity of electron-rich vinylarenes (Fig. 4a). For example, using 3-vinyl-*N*-Ts-indole as the substrate, under our standard conditions with the application of a cell voltage of 2.3 V ($E_{\text{anode}} \approx 0.24\text{ V}$ versus $\text{Fc}^{+/0}$), we observed full conversion of the alkene but minimal formation of the desired nitrile **20**. Instead, several side products were formed, including those that arose from over-oxidation of the benzyl radical intermediate⁵⁶ to the corresponding cation followed by nucleophilic trapping (for example, formate and ketone products). By lowering the voltage input from 2.3 V to 1.8 V ($E_{\text{anode}} \approx 0.08\text{ V}$), we successfully suppressed over-oxidation and obtained hydrocyanation product **20** in 71% yield. This principle was also applied to the optimization of reactions forming **8** and **59**.

For comparative purposes, we examined the hydrocyanation of alkene **1** under traditional chemical conditions without an electrical input. None of the chemical oxidants we surveyed promoted the reaction with efficiencies or enantioselectivities comparable to

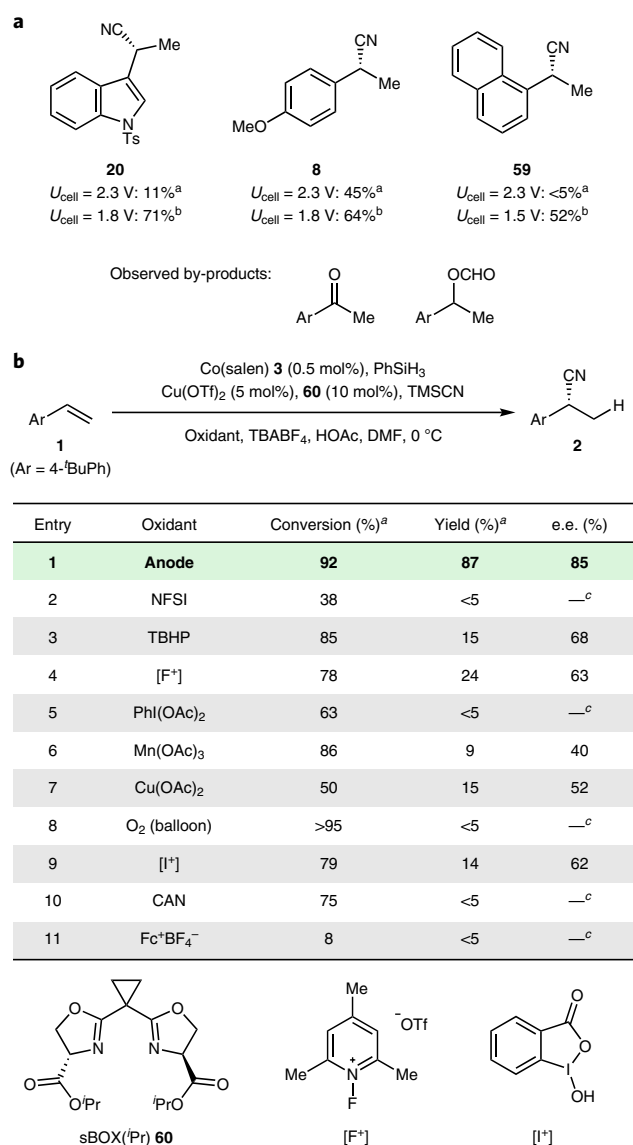


Fig. 4 | Electrochemical tuning of reaction chemoselectivity

and comparison with chemical methods. **a**, Reaction yield and chemoselectivity can be improved by lowering applied potential, minimizing by-products formation from overoxidation of electron-rich substrates. ^aDetermined by ¹H NMR. ^bIsolated yield. **b**, Control experiments show that common chemical oxidants in lieu of anodic oxidation cannot provide same levels of reactivity or enantioselectivity. ^cNot determined. NFSI, *N*-fluorobenzenesulfonamide; TBHP, *tert*-butyl hydroperoxide; CAN, ceric ammonium nitrate.

our protocol (Fig. 4b). In cases where a low yield of **2** was obtained (9–24%), the enantioselectivity was also substantially lower (40–68% e.e.). This erosion of e.e. is likely a result of a racemic carbocation pathway caused by over-oxidation of the key benzylic radical intermediate. We note that, although these results could potentially be improved through extensive optimization of reaction conditions, such optimization studies would need to address the challenges associated with the use of a terminal chemical oxidant. Electrochemistry, with its ability to enable electron transfer with a minimally sufficient potential input, provides an ideal means to circumvent issues with chemical oxidation and harness multiple redox catalytic cycles for productive chemistry.

Stereochemical model. Finally, we enlisted theoretical methods to elucidate the role played by sBOX ligands in directing the highly enantioselective Cu-mediated hydrocyanation. A previous study showed that the radical combination to generate intermediate **II** (Fig. 2) is facile, whereas reductive elimination to construct the C–CN bond is slow and thus enantio-determining³⁹. Traditionally, BOX-type ligands are thought to induce enantioselectivity through primarily repulsive steric interactions imparted by the bulky substituents on the oxazoline groups⁴⁹. Considering that the ester-derived ligands (**4**, **60**) perform substantially better than the canonical BOX ligands with various steric profiles (for example, **5**–**7**), we hypothesized that the ester groups must also provide attractive interactions with the substrate assembly in the key C–CN-forming transition state (TS). DFT computations are fully consistent with this hypothesis (Fig. 5 and Supplementary Information Section 7). Using the reaction that forms **10** as an example, the lowest-energy TS structures leading to the major (*R*) and minor (*S*) products (TS_{*R*} and TS_{*S*}, respectively) both display a favourable C–H••• π interaction between the acidic proton at the α -position of one ester group and the substrate aryl group. This attractive non-covalent interaction dictates the TS geometry by positioning the substrate alkyl group towards the ester on the opposite half of the catalyst. However, this arrangement causes more severe steric interactions in TS_{*S*} than TS_{*R*}. In addition to having the closest catalyst–substrate contacts (d_3 in Fig. 5), these exponentially repulsive steric interactions also force the bulky ^tBu-ester group to deviate more substantially from its optimal planar geometry in TS_{*S*} (both θ values in Fig. 5), and this broken conjugation further destabilizes the minor TS (Supplementary Information Section 11). Based on these findings, we further hypothesize that this complex interplay between attractive and repulsive non-covalent interactions in the TS determines the reaction enantioselectivity. We note in passing that this computational analysis refutes our previous hypothesis⁴⁵ that direct coordination of the ester groups to the Cu centre was responsible for stabilizing the major TS during enantioselective C–CN formation.

This stereochemical model is consistent with our experimental observations. For example, reactions with internal alkenes are in general more enantioselective than those with terminal alkenes. This can be explained by the increased steric interactions between the substrate alkyl group and the catalyst ester group in TS_{*S*} for the internal alkenes. In addition, substrates with more electron-rich aryl groups (for example, **2**, **8**) in general lead to higher enantioselectivity than those with electron-deficient groups (for example, **9**, **13**), which can be rationalized by an enhanced C–H••• π interaction with the aryl group⁵⁷.

Conclusions

The electrocatalytic hydrocyanation described herein reveals the unique advantages of harnessing electrochemistry in exploring new chemical space and developing solutions to challenging synthetic problems. This new transformation will enhance chemists' access to a diverse array of enantio-enriched nitriles. On a fundamental level, the realization of electrochemical hydrofunctionalization and demonstration of enantioselective electrocatalysis will improve the scope of electrosynthesis and its adoption in modern organic chemistry.

Online content

Any methods, additional references, Nature Research reporting summaries, source data, extended data, supplementary information, acknowledgements, peer review information; details of author contributions and competing interests; and statements of data and code availability are available at <https://doi.org/10.1038/s41557-020-0469-5>.

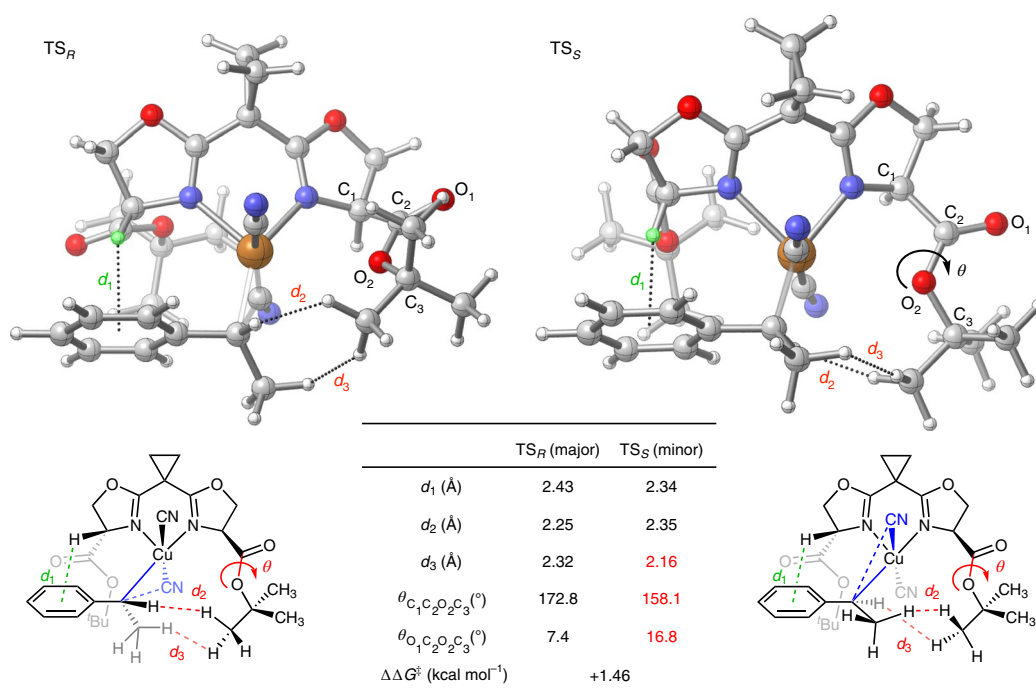


Fig. 5 | Computational stereochemical model. The minor and major TS for the reaction with ligand **4** and styrene (giving product **10**) are shown. DFT models show that the combination of an attractive C–H $\cdots\pi$ interaction between substrate and catalyst in conjunction with a sterically induced structural distortion of the catalyst determines the reaction enantioselectivity. Numbers in red indicate closest catalyst–substrate contacts or dihedral angles that substantially deviate from their optimal values.

Received: 16 September 2019; Accepted: 21 April 2020;
Published online: 29 June 2020

References

- Rajanbabu, T. V. Hydrocyanation of alkenes and alkynes. *Org. React.* **75**, 1–73 (2011).
- Nugent, W. A. & McKinney, R. J. Nickel-catalyzed Markovnikov addition of hydrogen cyanide to olefins. Application to nonsteroidal anti-inflammatory. *J. Org. Chem.* **50**, 5370–5372 (1985).
- Gaspar, B. & Carreira, E. M. Mild cobalt-catalyzed hydrocyanation of olefins with tosyl cyanide. *Angew. Chem. Int. Ed.* **46**, 4519–4522 (2007).
- Fang, X., Yu, P. & Morandi, B. Catalytic reversible alkene–nitrile interconversion through controllable transfer hydrocyanation. *Science* **351**, 832–836 (2016).
- Pollak, P., Romeder, G., Hagedorn, F. & Gelbke, H. *Ullman's Encyclopedia of Industrial Chemistry* 5th edn, Vol. A17 363 (Wiley-VCH, 1985).
- Tolman, C. A., McKinney, R. J., Seidel, W. C., Druliner, J. D. & Stevens, W. R. Homogeneous nickel-catalyzed olefin hydrocyanation. *Adv. Catal.* **33**, 1–46 (1985).
- Rajanbabu, T. V. & Casalnuovo, A. L. Tailored ligands for asymmetric catalysis. *J. Am. Chem. Soc.* **114**, 6265–6266 (1992).
- Rajanbabu, T. V. & Casalnuovo, A. L. Role of electronic asymmetry in the design of new ligands: the asymmetric hydrocyanation reaction. *J. Am. Chem. Soc.* **118**, 6325–6326 (1996).
- Casalnuovo, A. L., Rajanbabu, T. V., Ayers, T. A. & Warren, T. Ligand electronic effects in asymmetric catalysis: enhanced enantioselectivity in asymmetric hydrocyanation of vinylarenes. *J. Am. Chem. Soc.* **116**, 9869–9882 (1994).
- Kurono, N. & Ohkuma, T. Catalytic asymmetric cyanation reactions. *ACS Catal.* **6**, 989–1023 (2016).
- Bini, L., Müller, C. & Vogt, D. Ligand development in the Ni-catalyzed hydrocyanation of alkenes. *Chem. Commun.* **46**, 8325–8334 (2010).
- Saha, B. & Rajanbabu, T. V. Nickel(0)-catalyzed asymmetric hydrocyanation of 1,3-dienes. *Org. Lett.* **8**, 4657–4659 (2006).
- Falk, A., Göderz, A.-L. & Schmalz, H.-G. Enantioselective nickel-catalyzed hydrocyanation of vinylarenes using chiral phosphine–phosphite ligands and TMS–CN as a source of HCN. *Angew. Chem. Int. Ed.* **52**, 1576–1580 (2013).
- Falk, A., Cavalieri, A., Nichol, G. S., Vogt, D. & Schmalz, H.-G. Enantioselective nickel-catalyzed hydrocyanation using chiral phosphine–phosphite ligands: recent improvements and insights. *Adv. Synth. Catal.* **357**, 3317–3320 (2015).
- Wilting, J., Janssen, M., Müller, C. & Vogt, D. The enantioselective step in the nickel-catalyzed hydrocyanation of 1,3-cyclohexadiene. *J. Am. Chem. Soc.* **128**, 11374–11375 (2006).
- Li, X. et al. Asymmetric hydrocyanation of alkenes without HCN. *Angew. Chem. Int. Ed.* **58**, 10928–10931 (2019).
- Schuppe, A. W., Borraro-Calleja, G. M. & Buchwald, S. L. Enantioselective olefin hydrocyanation without cyanide. *J. Am. Chem. Soc.* **141**, 18668–18672 (2019).
- Francke, R. & Little, R. D. Redox catalysis in organic electrosynthesis: basic principles and recent developments. *Chem. Soc. Rev.* **43**, 2492–2521 (2014).
- Jutand, A. Contribution of electrochemistry to organometallic catalysis. *Chem. Rev.* **108**, 2300–2347 (2008).
- Meyer, T. H., Finger, L. H., Gandeepan, P. & Ackermann, L. Resource economy by metallaelectrocatalysis: merging electrochemistry and C–H activation. *Trends Chem.* **1**, 63–76 (2019).
- Yan, M., Kawamata, Y. & Baran, P. S. Synthetic organic electrochemical methods since 2000: on the verge of a renaissance. *Chem. Rev.* **117**, 113230–113319 (2017).
- Fu, N., Sauer, G. S., Saha, A., Loo, A. & Lin, S. Metal-catalyzed electrochemical diazidation of alkenes. *Science* **357**, 575–579 (2017).
- Ye, K. et al. Anodically coupled electrolysis for the heterodifunctionalization of alkenes. *J. Am. Chem. Soc.* **140**, 2438–2441 (2018).
- Fu, N. et al. Mn-catalyzed electrochemical chloroalkylation of alkenes. *ACS Catal.* **9**, 746–754 (2019).
- Zhu, L. et al. Electrocatalytic generation of amidyl radicals for olefin hydroamidation: use of solvent effects to enable anilide oxidation. *Angew. Chem. Int. Ed.* **55**, 2226–2229 (2016).
- Miranda, J. A., Wade, C. J. & Little, R. D. Indirect electroreductive cyclization and electrohydrocyclization using catalytic reduced nickel(II) salen. *J. Org. Chem.* **70**, 8017–8026 (2005).
- Shono, T. et al. Electroorganic chemistry. 118. Electroreductive intermolecular coupling of ketones with olefins. *J. Org. Chem.* **54**, 6001–6003 (1989).
- Lin, Q., Li, L. & Luo, S. Asymmetric electrochemical catalysis. *Chem. Eur. J.* **25**, 10033–10044 (2019).
- Nguyen, B. H., Redden, A. & Moeller, K. D. Sunlight, electrochemistry, and sustainable oxidation reactions. *Green Chem.* **16**, 69–72 (2014).
- Torii, S., Liu, P. & Tanaka, H. Electrochemical Os-catalyzed asymmetric dihydroxylation of olefins with Sharpless' ligand. *Chem. Lett.* **24**, 319–320 (1995).
- Crossley, S. W. M., Obradors, C., Martinez, R. M. & Shenvi, R. A. Mn-, Fe-, and Co-catalyzed radical hydrofunctionalizations of olefins. *Chem. Rev.* **116**, 8912–9000 (2016).

32. Isayama, S. & Mukaiyama, T. Hydration of olefins with molecular oxygen and triethylsilane catalyzed by bis-(trifluoroacetylacetonato)cobalt(II). *Chem. Lett.* **18**, 569–572 (1989).
33. Waser, J., Nambu, H. & Carreira, E. M. Cobalt-catalyzed hydroazidation of olefins: convenient access to alkyl azides. *J. Am. Chem. Soc.* **127**, 8294–8295 (2005).
34. Renata, H., Zhou, Q. & Baran, P. S. Strategic redox relay enables a scalable synthesis of ouabagenin, a bioactive cardenolide. *Science* **339**, 56–63 (2013).
35. Shigehisa, H. et al. Catalytic hydroamination of unactivated olefins using a Co catalyst for complex molecule synthesis. *J. Am. Chem. Soc.* **136**, 13534–13537 (2014).
36. Li, G., Han, A., Pulling, M. E., Estes, D. P. & Norton, J. R. Evidence for formation of a Co–H bond from $(\text{H}_2\text{O})_2\text{Co}(\text{dmgBF}_2)_2$ under H_2 : application to radical cyclizations. *J. Am. Chem. Soc.* **134**, 14662–14665 (2012).
37. Crossley, S. W. M., Barabé, F. & Shenvi, R. A. Simple, chemoselective, catalytic olefin isomerization. *J. Am. Chem. Soc.* **136**, 16788–16791 (2014).
38. King, S. M., Ma, X. & Herzon, S. B. A method for the selective hydrogenation of alkenyl halides to alkyl halides. *J. Am. Chem. Soc.* **136**, 6884–6887 (2014).
39. Zhang, W. et al. Enantioselective cyanation of benzylic C–H bonds via copper-catalyzed radical relay. *Science* **353**, 1014–1018 (2016).
40. Wang, F., Chen, P. & Liu, G. Copper-catalyzed radical relay for asymmetric radical transformations. *Acc. Chem. Res.* **51**, 2036–2046 (2018).
41. Gao, D.-W. et al. Direct access to versatile electrophiles via catalytic oxidative cyanation of alkenes. *J. Am. Chem. Soc.* **140**, 8069–8073 (2018).
42. Green, S. A., Matos, J. L. M., Yagi, A. & Shenvi, R. A. Branch-selective hydroarylation: iodoarene–olefin cross-coupling. *J. Am. Chem. Soc.* **138**, 12779–12782 (2016).
43. Discolo, C. A., Touney, E. E. & Pronin, S. V. Catalytic asymmetric radical–polar crossover hydroalkoxylation. *J. Am. Chem. Soc.* **141**, 17527–17532 (2019).
44. Zhang, G., Fu, L., Chen, P., Zou, J. & Liu, G. Proton-coupled electron transfer enables tandem radical relay for asymmetric copper-catalyzed phosphinoylcyanation of styrenes. *Org. Lett.* **21**, 5015–5020 (2019).
45. Fu, N. et al. New bisoxazoline ligands enable enantioselective electrocatalytic cyanofunctionalization of vinylarenes. *J. Am. Chem. Soc.* **141**, 14480–14485 (2019).
46. Shigehisa, H., Kikuchi, H. & Hiroya, K. Markovnikov-selective addition of fluororous solvents to unactivated olefins using a Co catalyst. *Chem. Pharm. Bull.* **64**, 371–374 (2016).
47. Eichhorn, E., Rieker, A. & Speiser, B. The electrochemical oxidation of $[\text{Co}^{\text{II}}(\text{salen})]$ in solvent mixtures—an example of a ladder scheme with coupled electron-transfer and solvent-exchange reactions. *Angew. Chem. Int. Ed.* **31**, 1215–1217 (1992).
48. Merchant, R. R. et al. Divergent synthesis of pyrone diterpenes via radical cross coupling. *J. Am. Chem. Soc.* **140**, 7462–7465 (2018).
49. Desimoni, G., Faita, G. & Jørgensen, K. A. Update 1 of: C_2 -symmetric chiral bis(oxazoline) ligands in asymmetric catalysis. *Chem. Rev.* **111**, PR284–PR437 (2011).
50. Zhu, R. & Buchwald, S. L. Versatile enantioselective synthesis of functionalized lactones via copper-catalyzed radical oxyfunctionalization of alkenes. *J. Am. Chem. Soc.* **137**, 8069–8077 (2015).
51. Zhang, Z., Stateman, L. M. & Nagib, D. A. δ C–H (hetero)arylation via Cu-catalyzed radical relay. *Chem. Sci.* **10**, 1207–1211 (2019).
52. Perrotta, D., Wang, M.-M. & Waser, J. Lewis acid catalyzed enantioselective desymmetrization of donor–acceptor meso-diaminocyclopropanes. *Angew. Chem. Int. Ed.* **57**, 5120–5123 (2018).
53. Redden, A. & Moeller, K. D. Anodic coupling reactions: exploring the generality of Curtin–Hammett controlled reactions. *Org. Lett.* **13**, 1678–1681 (2011).
54. Li, J. et al. Site-specific allylic C–H bond functionalization with a copper-bound N-centred radical. *Nature* **574**, 521–561 (2019).
55. He, G., Zhao, Y., Zhang, S., Lu, C. & Chen, G. Highly efficient syntheses of azetidines, pyrrolidines, and indolines via palladium catalyzed intramolecular amination of $C(\text{sp}^3)\text{--H}$ and $C(\text{sp}^2)\text{--H}$ bonds at γ and δ positions. *J. Am. Chem. Soc.* **134**, 3–6 (2012).
56. Wayner, D. D. M., McPhee, D. J. & Griller, D. Oxidation and reduction potentials of transient free radicals. *J. Am. Chem. Soc.* **110**, 132–137 (1988).
57. Bloom, J. W. G., Raju, R. K. & Wheeler, S. E. Physical nature of substituent effects in XH/π interactions. *J. Chem. Theory Comput.* **8**, 3167–3174 (2012).

Publisher's note Springer Nature remains neutral with regard to jurisdictional claims in published maps and institutional affiliations.

© The Author(s), under exclusive licence to Springer Nature Limited 2020

Methods

General procedure for the electrochemical hydrocyanation of alkenes using a custom-made cell (0.20 mmol scale). In a 2 dram vial, ligand **4** (7.6 mg, 0.02 mmol, 10 mol%) and Cu(OTf)₂ (3.6 mg, 0.01 mmol, 5 mol%) were dissolved in DMF (1.0 ml) under a N₂ atmosphere, and the mixture was stirred for 2 h before use (Solution A).³⁸ An oven-dried, 10 ml two-neck glass tube was equipped with a magnetic stir bar, a rubber septum, a threaded Teflon cap fitted with electrical feedthroughs, a carbon felt anode (1 × 0.5 × 0.6 cm³; connected to the electrical feedthrough via a graphite rod that was 9 cm in length and 2 mm in diameter) and a platinum plate cathode (1.0 × 0.5 cm²). To this reaction vessel, TBABF₄ (132 mg) was added. The cell was sealed and flushed with nitrogen gas for 5 min, followed by the sequential addition via syringe of the olefin substrate (0.2 mmol, 1.0 equiv., dissolved in 1 ml DMF) and HOAc (60 μl, 1 mmol, 5 equiv.), Co(salen) **3** (0.6 mg, 0.001 mmol, 0.5 mol%, dissolved in 1 ml DMF) and Solution A. A nitrogen-filled balloon was adapted through the septum to sustain a nitrogen atmosphere. The reaction vessel was then cooled to 0 °C. PhSiH₃ (24 mg, 0.22 mmol, 1.1 equiv.) and TMSCN (50 μl, 0.4 mmol, 2 equiv.) were dissolved in DMF (1.0 ml), and the resulting solution was added to the glass tube via syringe. Electrolysis was initiated at a cell potential of 2.3 V at 0 °C. Upon full consumption of the olefin starting material as determined by thin-layer chromatography analysis, the electrical input was removed. The mixture was diluted with ethyl acetate (60 ml) and then washed with water (40 ml) and brine, dried over anhydrous Na₂SO₄ and concentrated under reduced pressure. The residue was subjected to flash column chromatography on silica gel (eluted with hexanes and ethyl acetate) to yield the desired product. See Extended Data Fig. 1a.

General procedure for the electrochemical hydrocyanation of alkenes using ElectraSyn 2.0 (0.30 mmol scale). The graphite plate was removed from the ElectraSyn graphite electrode assembly to obtain the empty electrode holder and then a piece of carbon felt (5.3 × 0.8 × 0.6 cm³) was cut and fixed on the commercial graphite electrode using Pt wire as the working electrode. Pt foil was used as the counter electrode. In a dried sealed tube, sBOX(Pr) **60** (11.4 mg, 0.03 mmol) and Cu(OTf)₂ (5.4 mg, 0.015 mmol) were dissolved in DMF (1.0 ml) under a N₂ atmosphere, and the mixture was stirred for 2 h before use. The ElectraSyn vial (10 ml volume) was charged with a Teflon-coated magnetic stir bar, TBABF₄ (198 mg, 0.6 mmol) and olefin (48.0 mg, 0.30 mmol). The screw thread area of the vial was covered with a rubber septum to ensure that the seal was airtight. The carbon felt and Pt foil electrodes were adapted onto the ElectraSyn vial cap, the vial cap was screwed onto the vial to finger tightness and the vial was flushed with nitrogen gas for 5 min. Using a syringe, DMF (3.0 ml), HOAc (90 mg, 1.5 mmol), Co(salen) **3** (0.0015 mmol, 0.5 mol%, 0.9 mg dissolved in 1 ml DMF) and the copper catalyst solution (prepared as in the 0.20 mmol scale procedure) were added through the rubber septum. A nitrogen-filled balloon was adapted through the septum to sustain a nitrogen atmosphere. The electrochemical cell was adapted onto the vial holder of the ElectraSyn 2.0, and the reaction vessel was then cooled to 0 °C using an ice bath. After that, TMSCN (0.6 mmol, 75 μl) and PhSiH₃ (0.33 mmol, 35.7 mg) were dissolved in DMF (1.0 ml), which was added to the reaction solution via syringe. The settings 'new experiments' at 'constant current' were selected, and the current was adjusted to 3.0 mA. The settings 'No' for 'use of reference electrode' were selected, and the reaction time was adjusted to '10 h 43 min 35 sec'. The setting 'mmols substrate' was adjusted to '0.3 mmol' and the polarity was chosen not to alternate. After reviewing the parameters, the ice bath was removed and the experiment started. After electrolysis, the reaction vial was disconnected from the ElectraSyn 2.0, the cap with electrodes was gently removed from the vial and the reaction media was transferred to a separatory funnel. Both electrodes were washed with ethyl acetate (20 ml) to transfer any residual product. Then, 30 ml ethyl acetate was added to the separatory funnel, and the organic solution was washed with water and brine. The organic layer was dried with anhydrous Na₂SO₄ and concentrated under reduced pressure. The residue was subjected to flash column chromatography on silica gel (eluted with hexanes and ethyl acetate) to yield 32.0 mg of the desired product (57% yield, 73% based on recovered starting material, unoptimized) with 86% e.e. See Extended Data Fig. 1b.

Scale-up electrolysis using a commercial three-necked flask (2.0 mmol, 0.4 g scale). In a dried sealed tube, sBOX(Bu) **4** (76.0 mg, 0.2 mmol) and Cu(OTf)₂ (36.1 mg, 0.1 mmol) were dissolved in DMF (4.0 ml) under a N₂ atmosphere, and the mixture was stirred for 2 h before use. To an oven-dried three-neck round-bottom flask (50 ml) equipped with a magnetic stir bar were added TBABF₄ (988 mg, 3 mmol) and olefin substrate (368.4 mg, 2 mmol). Each neck was fitted with a rubber septum. The septa on the side necks were fitted with a carbon felt anode (1.5 × 1.0 × 0.6 cm³; connected to a graphite rod that was 9 cm in length and 2 mm in diameter) and a platinum foil cathode (2.5 × 1.5 cm²), with the lower (closest) ends of the electrodes 0.5 cm apart. The cell was sealed and flushed with nitrogen gas for 5 min, followed by the addition via syringe of DMF (24 ml), HOAc (0.6 ml), Co(salen) **3** (0.01 mmol, 0.5 mol%, 6.0 mg dissolved in 1 ml DMF) and copper catalyst solution made in advance. A nitrogen-filled balloon was adapted through the septum to sustain a nitrogen atmosphere. The reaction vessel was then cooled to 0 °C. After that, TMSCN (4 mmol, 2 equiv., 500 μl) and PhSiH₃ (2.2 mmol, 1.1 equiv., 238 mg) were dissolved in DMF (1.0 ml) and added to the reaction

solution via syringe. Electrolysis was initiated at a constant current of 7.0 mA at 0 °C. Reaction was stopped after 4.0 F mol⁻¹ charge was passed (30 h 38 min). The mixture was then diluted with ethyl acetate (200 ml) and then washed with water and brine, dried over anhydrous Na₂SO₄ and concentrated under reduced pressure. The residue was subjected to flash column chromatography on silica gel (eluted with hexanes and ethyl acetate) to yield 299.9 mg of the desired product (71% yield) with 90% e.e. See Extended Data Fig. 1c.

Scale-up electrolysis using a commercial three-necked flask (5.0 mmol, 0.8 g scale). In a dried sealed tube, sBOX(Bu) **4** (190.0 mg, 0.5 mmol) and Cu(OTf)₂ (90.4 mg, 0.25 mmol) were dissolved in DMF (10.0 ml) under a N₂ atmosphere, and the mixture was stirred for 2 h before use. To an oven-dried three-neck round-bottom flask (100 ml) equipped with a magnetic stir bar were added TBABF₄ (1.98 g, 6 mmol) and olefin substrate (800 mg, 5 mmol). Each neck was fitted with a rubber septum. The septa on the side necks were fitted with a carbon felt anode (1.8 × 1.8 × 0.6 cm³; connected to a graphite rod that was 9 cm in length and 2 mm in diameter) and a platinum foil cathode (2.0 × 3.0 cm²), with the lower (closest) ends of the electrodes 1.0 cm apart. The cell was sealed and flushed with nitrogen gas for 5 min, followed by the addition via syringe of DMF (35 ml), HOAc (1.5 ml), Co(salen) **3** (0.025 mmol, 0.5 mol%, 15 mg dissolved in 10 ml DMF) and copper catalyst solution made in advance. A nitrogen-filled balloon was adapted through the septum to sustain a nitrogen atmosphere. The reaction vessel was then cooled to 0 °C. After that, TMSCN (10 mmol, 2 equiv., 1,250 μl) and PhSiH₃ (5.5 mmol, 1.1 equiv., 594 mg) were dissolved in DMF (5.0 ml) and added to the reaction solution via syringe. Electrolysis was initiated at a constant current of 10.0 mA at 0 °C. Reaction was stopped after 4.0 F mol⁻¹ charge was passed (53 h 37 min). The mixture was then diluted with ethyl acetate (300 ml) and then washed with water and brine, dried over anhydrous Na₂SO₄ and concentrated under reduced pressure. The residue was subjected to flash column chromatography on silica gel (eluted with hexanes and ethyl acetate) to yield 514.2 mg of desired product (55% yield) with 85% e.e. See Extended Data Fig. 1d.

General procedure for control experiments using chemical oxidants instead electrochemistry. In a 2 dram vial, sBOX(Pr) (3.5 mg, 0.01 mmol, 10 mol%) and Cu(OTf)₂ (1.8 mg, 0.005 mmol, 5 mol%) were dissolved in DMF (1.0 ml) under a N₂ atmosphere, and the mixture was stirred for 2 h before use. To a dried 2 dram vial, *tert*-butylstyrene (16.0 mg, 0.1 mmol, 1.0 equiv.), the oxidant (0.1 mmol, 1.0 equiv.) and HOAc (30.0 mg, 0.5 mmol, 5.0 equiv.) were added under a N₂ atmosphere. After that, Co(salen) (0.0005 mmol, 0.5 mol%, 0.3 mg dissolved in 0.5 ml DMF) and the copper catalyst solution made in advance were added. A nitrogen-filled balloon was adapted through the septum to sustain a nitrogen atmosphere. The reaction vessel was then cooled to 0 °C. PhSiH₃ (0.11 mmol, 1.1 equiv., 12 mg) and TMSCN (0.2 mmol, 2 equiv., 25 μl) were dissolved in DMF (0.5 ml) and added to the reaction solution via syringe. After stirring at room temperature for 24 h, the mixture was diluted with ethyl acetate (20 ml) and then washed with water and brine, dried over anhydrous Na₂SO₄ and concentrated under reduced pressure. Yields were determined with ¹H NMR analysis using 1,3,5-trimethoxybenzene as the internal standard. The e.e. value of the product was measured by HPLC analysis on a chiral stationary phase.

Product derivatization: nitrile methanolysis. In a dried sealed tube, (*R*)-2-(6-methoxynaphthalen-2-yl)propanenitrile **15** (21.1 mg, 0.10 mmol, 90% e.e.) and 37% HCl (1.0 ml) were dissolved in MeOH (1.0 ml) under a N₂ atmosphere. The mixture was then heated at 80 °C for 48 h. After cooling to room temperature, the mixture was extracted with ethyl acetate (30 ml) three times. The combined organic layers were dried over anhydrous Na₂SO₄ and concentrated under vacuum. Column chromatography using silica gel was then applied to yield the desired product in 62% yield (15.1 mg) in 90% e.e. as a colourless oil. See Extended Data Fig. 2a.

Product derivatization: indoline formation. For step 1, a solution of (*R*)-2-(6-methoxynaphthalen-2-yl)propanenitrile **15** (0.3 mmol, 63.3 mg, 90% e.e.) and CoCl₂ (0.6 mmol, 2.0 equiv., 78 mg) in dry methanol (3.0 ml) was cooled to 0 °C under a nitrogen atmosphere. NaBH₄ (3.0 mmol, 10 equiv., 114 mg) was added in portions. The resulting reaction mixture was then allowed to warm to room temperature and continued to be stirred for 2 h. After that, the reaction mixture was poured into 100 ml of 2 M HCl at 0 °C and stirred until the black precipitate was dissolved. The mixture was washed with ethyl acetate (50 ml) three times, and the aqueous layer was made alkaline with NaOH at 0 °C and then extracted with ethyl acetate (100 ml) twice. The organic layer was separated and dried over Na₂SO₄, filtered and concentrated in vacuo. The crude product with 84% yield was used directly for the next step.

For step 2, under a N₂ atmosphere, a solution of **S1** (43.0 mg, 0.2 mmol), picolinic acid (29.5 mg, 1.2 equiv., 0.24 mmol), EDC (57.5 mg, 1.5 equiv., 0.3 mmol) and DMAP (2.5 mg, 0.1 equiv., 0.02 mmol) in dry dichloromethane (2.0 ml) was stirred at room temperature overnight. After that, the reaction mixture was purified directly by flash column chromatography to give the desired product with 80% isolated yield. See Extended Data Fig. 2b.

For step 3, under a N₂ atmosphere, a mixture of **S2** (0.1 mmol, 1.0 equiv., 32 mg), Pd(OAc)₂ (0.005 mmol, 0.05 equiv., 1.2 mg), PhI(OAc)₂ (0.25 mmol, 2.5 equiv., 80.5 mg) and toluene (1 ml) in a sealed tube was heated at 60 °C for 24 h. The reaction mixture was cooled to room temperature and concentrated under reduced pressure. The resulting residue was purified by silica gel flash chromatography to give the cyclized product with 92% isolated yield in 90% e.e.

Product derivatization: dihydroisoquinolinone formation. Under a N₂ atmosphere, a solution of methyl (*R*)-2-(1-cyanoethyl)benzoate **18** (0.1 mmol, 18.9 mg, 85% e.e.) and CoCl₂ (0.2 mmol, 2.0 equiv., 26 mg) in dry methanol (1.0 ml) was cooled to 0 °C. NaBH₄ (1.0 mmol, 10 equiv., 38 mg) was added in portions. The resulting reaction mixture was then allowed to warm to room temperature and continued to be stirred for 2 h. After that, the reaction mixture was heated to reflux overnight. The resulting reaction mixture was extracted by ethyl acetate (20 ml) three times, and the combined organic layers were dried over anhydrous Na₂SO₄. Purification by silica gel flash chromatography gave the cyclized product with 81% isolated yield in 87% e.e. See Extended Data Fig. 2c.

Computational details. All geometries were optimized using the ωB97X-D^{59,60} density functional approximation with the 6-31G* basis set in the Q-Chem software package⁶¹, with single-point electronic energy corrections obtained at the ωB97X-V level of theory⁶² with the def2-TZVPPD basis set⁶³ on the Cu atom and aug-cc-pVTZ⁶⁴ on all other atoms in the Psi4 software package⁶⁵. Rotations about the carbon–ester bond (C₁–C₂ in Fig. 5) and the Cu–substrate bond, as well as various different axial/equatorial Cu–ligand coordination geometries, were sampled as starting points for geometry optimizations during the searches for the global energy minima of the catalytic intermediates. The frozen string algorithm^{66,67} was also used as an aid during transition state searches. Analytical vibrational frequencies confirmed the nature of all stationary points, wherein transition state structures each contained a single imaginary frequency connecting the catalytic intermediate structure and the corresponding product. Thermal contributions to the free energy were computed at 273.15 K using partition functions derived within the ideal gas, rigid rotor, and harmonic oscillator approximations. See Extended Data Fig. 2.

Data availability

The data that support the findings of this study are included in this published article and its Supplementary Information files. Crystallographic data for compound **4** has been deposited at the Cambridge Crystallographic Data Centre under deposition number 1978310 and can be obtained free of charge (http://www.ccdc.cam.ac.uk/data_request/cif).

References

58. Fu, N., Sauer, G. S. & Lin, S. A general, electrocatalytic approach to the synthesis of vicinal diamines. *Nat. Protoc.* **13**, 1725–1743 (2018).
59. Chai, J.-D. & Head-Gordon, M. Long-range corrected hybrid density functionals with damped atom–atom dispersion corrections. *Phys. Chem. Chem. Phys.* **10**, 6615–6620 (2008).

60. Grimme, S. Semiempirical GGA-type density functional constructed with a long-range dispersion correction. *J. Comput. Chem.* **27**, 1787–1799 (2006).
61. Shao, Y. et al. Advances in molecular quantum chemistry contained in the Q-Chem 4 program package. *Mol. Phys.* **113**, 184–215 (2015).
62. Mardirossian, N. & Head-Gordon, M. ωB97X-V: A 10-parameter, range-separated hybrid, generalized gradient approximation density functional with nonlocal correlation, designed by a survival-of-the-fittest strategy. *Phys. Chem. Chem. Phys.* **16**, 9904–9924 (2014).
63. Rappoport, D. & Furche, F. Property-optimized Gaussian basis sets for molecular response calculations. *J. Chem. Phys.* **133**, 134105 (2010).
64. Dunning, T. H. Gaussian basis sets for use in correlated molecular calculations. I. The atoms boron through neon and hydrogen. *J. Chem. Phys.* **90**, 1007–1023 (1989).
65. Parrish, R. M. et al. Psi4 1.1: An open-source electronic structure program emphasizing automation, advanced libraries, and interoperability. *J. Chem. Theory Comput.* **13**, 3185–3197 (2017).
66. Behn, A., Zimmerman, P. M., Bell, A. T. & Head-Gordon, M. Efficient exploration of reaction paths via a freezing string method. *J. Chem. Phys.* **135**, 224108 (2011).
67. Sharada, S. M., Zimmerman, P. M., Bell, A. T. & Head-Gordon, M. Automated transition state searches without evaluating the Hessian. *J. Chem. Theory Comput.* **8**, 5166–5174 (2012).

Acknowledgements

Financial support to S.L. was provided by NIGMS (R01GM130928) and Eli Lilly. Financial support to B.G.E. and R.A.D. was provided by start-up funding from Cornell University. This study made use of the NMR facility supported by the NSF (CHE-1531632) and resources of the National Energy Research Scientific Computing Center (NERSC), a US Department of Energy Office of Science User Facility operated under contract no. DE-AC02-05CH11231. We thank K. Moeller for helpful discussions, A. Condo for gas chromatography mass spectrometry analysis, Y. Shen and J. Liu for providing some of the substrates and IKA for donation of the ElectraSyn 2.0.

Author contributions

S.L. conceived of the project. L.S., N.F., M.O.F. and S.L. designed the experiments. L.S., N.F. and W.H.L. carried out the experiments. B.G.E. and R.A.D. designed and carried out all DFT calculations. B.G.E., R.A.D. and S.L. analysed the DFT data. All authors contributed to writing the manuscript.

Competing interests

The authors declare no competing interests.

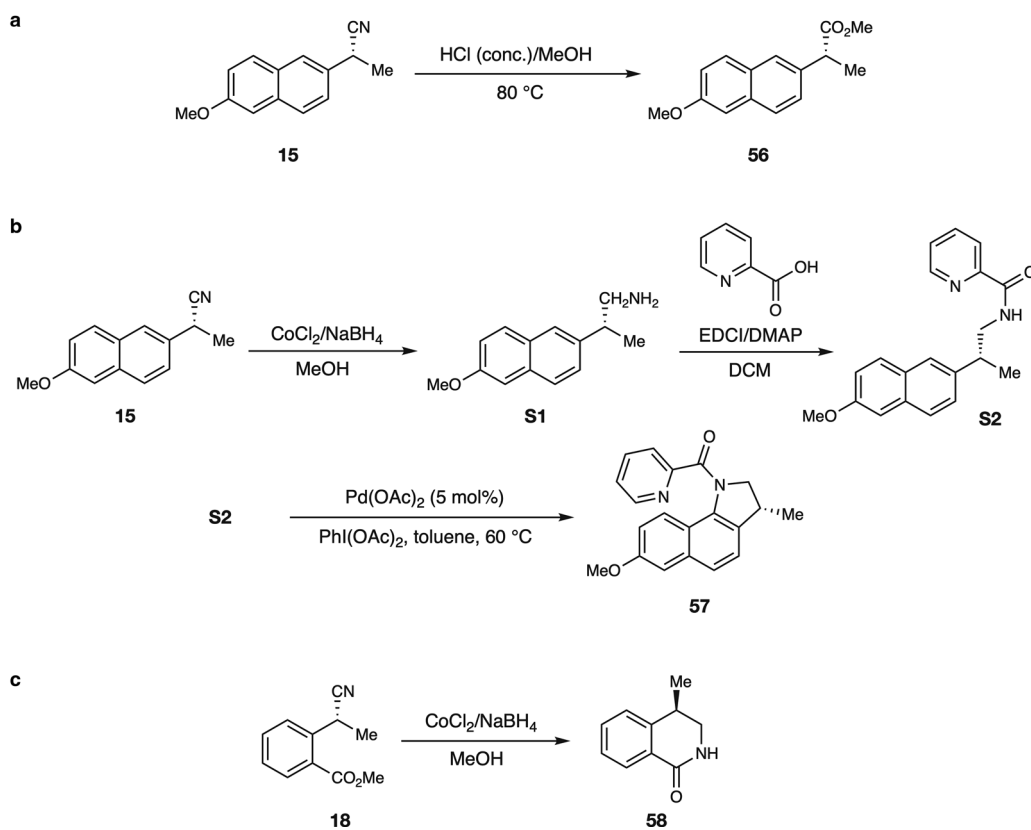
Additional information

Extended data is available for this paper at <https://doi.org/10.1038/s41557-020-0469-5>.

Supplementary information is available for this paper at <https://doi.org/10.1038/s41557-020-0469-5>.

Correspondence and requests for materials should be addressed to R.A.D. or S.L.

Reprints and permissions information is available at www.nature.com/reprints.



Extended Data Fig. 2 | Methods for product derivatization. **a**, Derivatization of product **15** to naproxen methyl ester **56** (analogue of naproxen). **b**, Derivatization of product **15** to benzoinoline **57** (analogue of duocarmycin). **c**, Derivatization of product **18** to dihydroisoquinolone **58** (analogue of palonosetron). Detailed experimental procedures can be found in Methods section.